

**Particle transport in asymmetric scanning-line optical tweezers**

B. Liesfeld,\* R. Nambiar,† and J. C. Meiners‡

*Department of Physics and Biophysics Research Division, University of Michigan, Ann Arbor, Michigan 48109-1120, USA*

(Received 19 December 2002; revised manuscript received 2 May 2003; published 24 November 2003)

We describe a scanning-line optical tweezing technique with an asymmetric beam profile in the back focal plane of the microscope objective. The motion of a trapped particle along the scan line is studied as a function of beam asymmetry, and it is shown that this technique can be used to exert a constant lateral force on the particle, realizing purely optical constant-force tweezing. The observed effect is attributed in a geometric optics model to a non-zero lateral component of the scattering force.

DOI: 10.1103/PhysRevE.68.051907

PACS number(s): 87.80.Cc

**I. INTRODUCTION**

Over the past decade optical tweezers have become an increasingly powerful tool for the study of biomolecules and colloidal systems. In most experimental configurations, a tightly focused laser beam is used to trap a microscopic particle through optical gradient forces in a harmonic potential in all three dimensions. Such an optical trap is relatively stiff, with a lateral spring constant of the order of 100 pN/ $\mu\text{m}$ , which exceeds by far the stiffness of most biomolecules that are studied with these instruments, such as viral DNA molecules under moderate tension [1] or single titin molecules [2]. Therefore, measurements with such a stationary trap are effectively imposing constant-extension conditions upon the molecule, providing for experiments where force is measured as a function of extension.

For numerous applications, however, a mode in which the molecule is held with a constant force regardless of its extension is necessary. Prime examples for such applications are studies of motor proteins that move processively along the DNA strand, such as RNA polymerases [3] or phage-head packing motors [4]. Conventional optical tweezers can be operated in a constant-force mode by using a feedback mechanism, which tracks the motion of the trapped particle by moving the focus of the laser beam or the distant attachment point of the molecule in such a fashion that the average displacement of the particle from the center of the trap remains constant [5]. Such an active feedback trap requires rather elaborate feedback electronics and operates well only at higher loads. Furthermore, this kind of feedback is rather slow and provides only average constant-force conditions, but cannot respond quickly to fast individual events such as a single step of a motor molecule. For experiments in the low-force or even zero-force regime or experiments with high temporal resolution, another method is required.

In this paper, we show that scanning-line optical tweezers with an asymmetric beam profile in the back focal plane of the microscope objective can be used to exert small, approxi-

mately constant, lateral radiation pressure forces on a trapped particle over a distance of several microns, thus eliminating the need for feedback mechanisms.

Scanning-line optical tweezers scan the focus of the trapping laser beam rapidly along a line in the focal plane of the microscope objective. The resultant optical gradient forces effectively trap the particle in the two dimensions perpendicular to the scan line, while allowing it to move with relative ease along this line. A number of experiments have used this technique to create very shallow one-dimensional potential wells, where the trapped particle “sees” only an effective potential that is determined by the time average of the light intensity at any spot along the scan line. In this manner Crocker *et al.* have measured entropic interactions in binary colloids [6], interaction potentials between polymer-coated microspheres [7], and attractions between colloidal particles in polymer solutions [8].

These experiments were static in nature, and considered only the time average of the optical potential. There is, however, a wealth of dynamic phenomena that can be observed with scanning line optical tweezers once the time dependence of the optical potential is fully taken into account. Faucheux *et al.* demonstrated that a stationary but time-dependent asymmetric potential along the scan line acts as a thermal ratchet [9]. Faucheux *et al.* have also experimentally studied the motion of a particle in symmetric scanning-line optical tweezers [10]. They found three different regimes, depending on the velocity of the scan. At low velocities, the particle remains trapped, at intermediate velocities it moves briefly in the direction of the scan and then escapes, and at high velocities the particle is in a diffusive regime where it moves freely along the scan line. They have also shown theoretically that for an arbitrary asymmetric one-dimensional potential in the focal plane the particle will always move in the direction of the scan, regardless of the exact shape of the potential.

In our study we show that an asymmetry in the beam profile in the back focal plane of the microscope objective has a markedly different effect than such an asymmetry in the focal plane. Most notably, the particle moves in the direction where the trap is weakest, irrespective of the scan direction. To summarize our explanation of this effect, the asymmetry in the back focal plane causes an asymmetry in the backscattered light from the trapped particle. This, in turn, gives rise to a lateral component in the corresponding

\*Electronic address: ben.liesfeld@umich.edu

†Electronic address: rnambiar@umich.edu

‡Electronic address: meiners@umich.edu;

<http://www.physics.lsa.umich.edu/meiners>

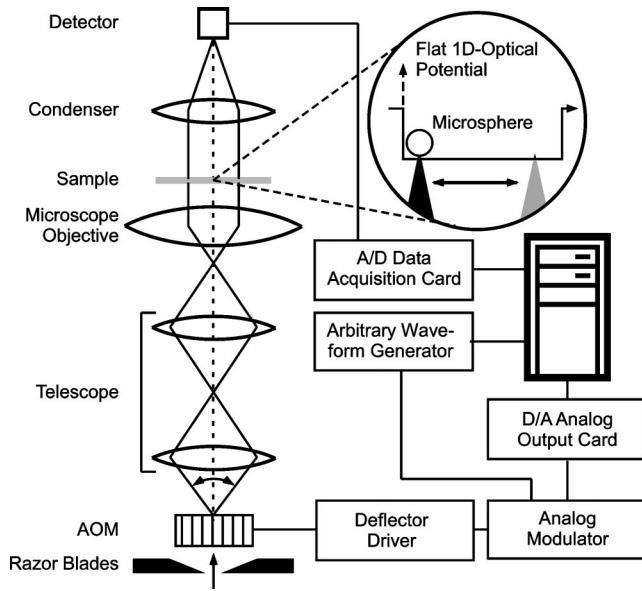


FIG. 1. Schematic setup of the scanning-line optical tweezers. A Gaussian laser beam is partially cut by a pair of knife edges and deflected by an acousto-optic modulator (AOM). The knife edges are imaged onto the back focal plane of a microscope objective, which focuses the beam into the sample cell. A condenser lens images the transmitted laser light onto a fast photodiode. The optical setup is supported by a computerized data acquisition system.

radiation pressure, exerting a net force on the particle in that direction regardless of the scanning motion.

## II. EXPERIMENTAL APPARATUS

Our scanning-line optical tweezer apparatus consists mainly of a Nd:YAG (yttrium aluminum garnet) laser ( $\lambda = 1064$  nm), an acousto-optic modulator (IntraAction Corp. Model DTD-274HA6), a telescope system, and a microscope objective (Zeiss Plan-Neofluoar 100X 1.3 oil), as shown in Fig. 1. The laser beam is deflected by the acousto-optic modulator, imaged onto a beam steering mirror, and imaged again onto the back focal plane of the microscope objective, where it has a typical intensity of 480 mW. The microscope objective focuses the laser beam to a diffraction-limited spot  $10 \mu\text{m}$  deep into the sample cell. A movable slit is placed in front of the acousto-optic modulator such that the telescopes image it onto the back focal plane. It is used to control the beam profile. The slit is wider than the beam at this point, enabling us to selectively cut off only one side of the Gaussian profile.

The sample cell consists of a microscope slide and a cover slip, separated by an approximately  $100 \mu\text{m}$  thick spacer. It is filled with an aqueous solution (1-mM NaCl ethylenediamine tetra-acetic acid 1-mM, 10-mM TrisCl, 0.1-mM Tween20;  $p\text{H}8.0$ ) of fluorescent polystyrene microspheres of  $1 \mu\text{m}$  diameter (Bangs Laboratories, Inc.) at an extremely low volume fraction ( $\Phi < 10^{-7}$ ). The cell is hermetically sealed with an epoxy glue to prevent evaporation and fluid flow. It is mounted on a translation stage that is actuated with a stepper motor (Newport PP-12) under computer control.

In order to measure the position of the microsphere in the optical potential, we collect the laser light that is transmitted through the sample cell on the other side with a condenser lens and image it onto a fast photodiode. When the laser beam hits the microsphere during the scan, the transmitted light intensity drops momentarily. From the timing of this dip, we can infer the position of the microsphere with an accuracy of about 50 nm each scan [11].

The optical system is controlled by a computerized signal generation and data acquisition system, as depicted in Fig. 1. A programmable arbitrary waveform generator (Tektronix AFG320) generates the frequency modulation signal for the RF driver (IntraAction Corp. Model DE-272M) of the acousto-optic modulator. The frequency modulation signal is a sawtooth function of 20 kHz that generates the scan. An additional electronic analog scaling and switching circuit is used to modify the amplitude and offset of the scan ramp. This allows us to position a particle that is trapped in the line potential by collapsing the scan into a single point. Subsequently, the particle can be released again into the line potential by switching back to full scan amplitude.

The data acquisition system consists of a fast photodiode mounted in the focal plane of the condenser lens, an amplifier with 10-MHz bandwidth, and a 14-bit analog-to-digital converter card with a sampling rate of 10-MHz (GageScope 14100). Acquisition of a 500-point data frame is triggered by the start of each scan. Up to 20000 frames were acquired each time a microsphere was released into the line potential, covering 0.2 s. The data are stored and analyzed off line to yield the position of the particle as a function of time upon release into the line potential. In addition, we monitor the position of the microsphere optically through epifluorescence microscopy. The images are acquired with a commercial charge-coupled device camera and digitized with a frame grabber card for subsequent off-line video analysis.

## III. RESULTS AND DISCUSSION

The principal aim of this study is to probe the particle transport in an optical line potential created by scanning a beam that is asymmetric in the back focal plane of the microscope objective. To this end, we positioned a microsphere with the optical trap in the middle of the scan line and released it. The motion of the microsphere was recorded by observing the transmitted laser light in the image plane of the condenser lens as previously described. This experiment was repeated for seven different positions of the beam-shaping slit in front of the acousto-optic modulator which lies in a plane conjugate to the back focal plane of the microscope objective. The fractional drop in intensity due to the partial blockage of the beam was measured for each position of the knife edges directly behind the slit. The overall laser power was then adjusted such that the integral intensity after the slit was the same for all measurements. The results are shown in Fig. 2(a). Upon release into the line potential, the microsphere moves at approximately constant velocity to one end of the scan line. The position of the beam-shaping slit determines the direction and velocity of this motion. If the beam entering the microscope objective is partially blocked on the

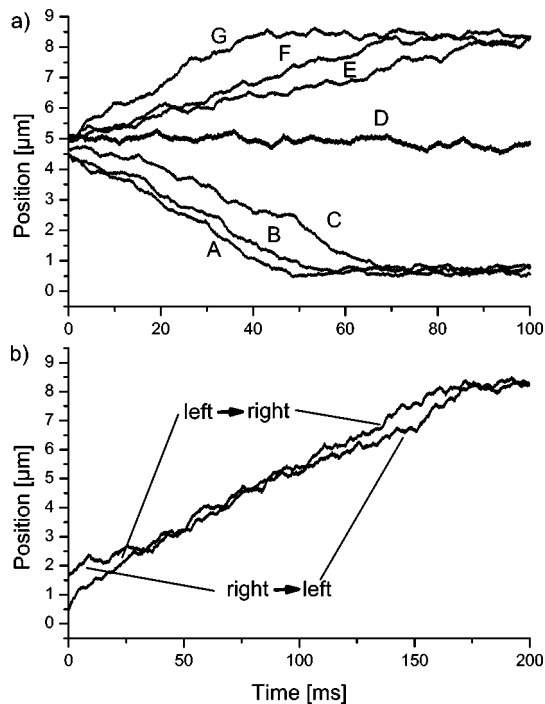


FIG. 2. Trajectories of a bead being released into the scanning line potential; (a) while blocking different parts of the laser beam in the back focal plane: A, B, and C blocking 30%, 25%, and 20% from the left, respectively; D not blocking the beam at all; E, F, and G blocking 20%, 25%, and 30% of the beam from the right. (b) Released into a potential while cutting 36% off the beam from the right side. The scan direction was reversed for the two traces as indicated.

left side, the particle moves to the left and vice versa. The velocity of the microsphere increases as the fractional blockage of the beam is increased. When more than 40% of the beam is blocked, however, we were unable to stably trap a particle in the line potential as the confinement in the axial direction becomes too weak.

In order to distinguish a transport caused by an asymmetry of the optical potential in the back focal plane from an effect caused by the reaction of the microsphere to the scanning motion of the trapping potential itself, we reversed the scan direction. Figure 2(b) shows that the particle still moves in the same direction at almost the same velocity, even though the direction of the scan has been reversed. This demonstrates that the motion of the optical potential and any possible asymmetries in that potential in the focal plane are not primarily responsible for the observed particle transport, as Faucheux *et al.* [10] have shown that a moving one-dimensional potential always leads to a net transport in the direction of the scanning motion, irrespective of the exact potential shape.

Following their argument, we look at the forces and resultant motion of a microsphere when it is subjected to the gradient forces of the scanned trap. These forces can be described as the derivative of a one-dimensional optical potential,  $F(x,t) = (-\partial/\partial x)U(x,t)$ , where the trap potential moves along the  $x$  axis at a velocity  $v$ , i.e.,  $U(x,t) = U(x - vt)$ . If the microsphere was stationary, as in the limit of an

infinite hydrodynamic friction coefficient of the particle, the impulse  $\int F(t)dt$  that acts on the particle each scan vanishes, as  $U(-\infty) = U(\infty)$ . When the microsphere reacts to the force, however, the time it moves towards the center of the laser beam against the direction of the scan is shortened, while the time it moves away from it is extended. Therefore, the impulse and the net displacement of the particle are positive for  $v > 0$  and negative for  $v < 0$ . Therefore, the particle will always move in the direction of the scan, which is contrary to our experimental observation. This effect, however, can explain the slight change in particle velocity upon reversal of the scan direction [seen in Fig. 2(b)]. Furthermore, the net displacement of the sphere per scan scales asymptotically as  $v^{-2}$  in the model of Faucheux *et al.* [10], and we therefore expect the particle velocity to be inversely proportional to the scan frequency. In our experiment the particle velocity depends only weakly on the scan frequency, as long as the scan rate is well above the escape velocity of the trap. The generally small difference in particle velocity upon reversal of the scan direction, however, exhibits a frequency dependence consistent with this model (data not shown).

Inertial effects that take the mass of the particle into account complicate this analysis, and we have performed additional numerical calculations for our experimental parameters to gauge their importance. These calculations show that inertial effects are extremely small compared to the forces and velocities observed or calculated in the simpler model above. Thus we conclude that scan direction and frequency independent motion of the particle cannot be attributed to the moving optical potential in the focal plane of the objective.

Another effect that can possibly lead to the observed particle transport might be a change in the optical gradient force as the laser focus moves along the scan line. Such a position-dependent change in the spring constant of the trap can be caused by a frequency dependence of the diffraction efficiency of the acousto-optic modulator, changes in intensity as the laser beam passes through the subsequent optical elements, and imaging errors such as geometrical aberrations.

In order to determine whether such effects cause indeed the observed behavior, we measured the lateral stiffness of a stationary trap at different positions along the scan line for different beam asymmetries. For this aim, a known viscous drag force was applied to the trapped microsphere by moving the sample cell at a constant velocity in the direction of the scan line. The displacement of the particle with respect to its equilibrium position in the trap was measured by video microscopy at a velocity of  $100 \mu\text{m/s}$  which corresponds to a friction force of  $\approx 1.0 \text{ pN}$ . The intensity of the laser beam was attenuated about eightfold to  $\approx 60 \text{ mW}$  at the back focal plane irrespective of the chosen beam asymmetry. This reduction in power approximates the average power the particle “sees” during a scan. The measurement was repeated for nine different positions of the stationary trap on the scan line for five different beam profiles in the back focal plane of the microscope objective [corresponding to B, D, and F in Fig. 2(a), as well as for a 49% cut, where the trap was just marginally stable]. In addition, reversal of the fluid flow allowed us to determine the asymmetry of the trap. The results are shown in Fig. 3(a).

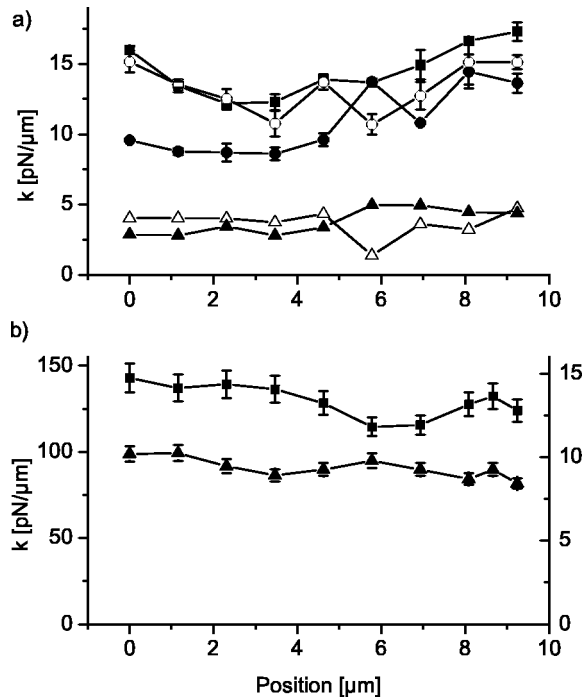


FIG. 3. Trap stiffness  $k$  as a function of position across the scan line for different beam profiles, acquired using different techniques. (a) Viscous drag method: squares denote measurements taken without cutting the beam. Circles denote data taken while cutting the beam by 25% from the left (filled symbols) and from the right (open symbols), respectively. Triangles denote data taken while cutting 49% off the beam. The laser power was attenuated approximately eightfold. (b) Brownian motion: trap stiffness in lateral direction (squares, left scale) and in axial direction (triangles, right scale).

While the data show some systematic variations of the lateral trap stiffness across the scan line, this cannot explain the observed particle transport that we described earlier. In particular, the sign of the overall slope of the trap stiffness as a function of position does not reverse when the side from which the beam is cut is changed. Such a reversal in slope, however, would be required to explain why the direction of the particle transport reverses when the beam asymmetry is reversed, as seen in Fig. 2(a). Furthermore, we observe that the trap stiffness decreases appreciably only in the limit of a very unstable trap, i.e., when 49% of the beam is cut off. This, again, is inconsistent with the fact that the transport velocity increases when the beam becomes more asymmetric. If the position dependence of the trap stiffness was the cause of this effect, an increase in the slope of the trap stiffness as a function of position as the asymmetry is increased would be required. The data in Fig. 3(a) show absolutely no evidence of such an increase in slope for the larger beam asymmetries.

In addition, we noticed that the exact shapes of the curves in Fig. 3(a) strongly depend on the alignment of the acousto-optical modulator, while the particle transport shown in Fig. 2 is very reproducible. In particular, the reversal of the scan direction when the beam asymmetry is reversed is observed even in a grossly misaligned system, suggesting very

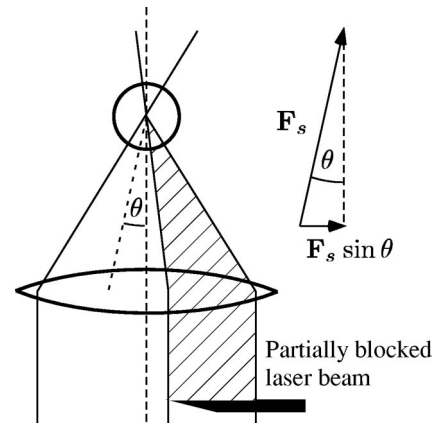


FIG. 4. Ray optics model to estimate the order of magnitude of the lateral component of the scattering force. When the laser beam is partially blocked, it hits the microsphere no longer orthogonally to the scan line, but under a small angle  $\theta$ . The force corresponding to the radiation pressure of the back reflection from the microsphere has now a lateral component  $F_s \sin \theta$ , which in turn moves the particle to the side where the beam is blocked.

strongly that the particle transport is not related to the change in lateral trap stiffness across the scan line.

To further independently characterize the position dependence of the trap stiffness not only in the lateral but also in the axial direction, we observed the Brownian motion of a particle in the harmonic potential of the stationary trap for different positions along the scan line at full laser power. For this aim, the photodiode in the focal plane of the condenser lens was replaced by a split photodiode. Position data were acquired at a rate of 100 kHz for several seconds, and the time-correlation function computed. A least-square fit to a double exponential decay yields the time constants for the lateral and axial motions of the particle in the trap, respectively [12]. The corresponding spring constants  $k$  of the trap are obtained from  $\tau = \zeta/k$ , where  $\tau$  is the lateral or axial time constant and  $\zeta$  the friction coefficient of the microsphere. The data shown in Fig. 3(b) exhibit the same slight decrease of trap stiffness on the right side of the scan line as in the viscous drag force measurements.

We therefore propose a different model to explain the scan direction and velocity independent particle transport that attributes it to a lateral component in the scattering force. When the laser beam hits the microsphere, a small portion of the beam is reflected. This reflection gives rise to radiation pressure and in turn a force acting on the particle. If the beam is perfectly symmetric, this force acts in the axial direction perpendicular to the scan line, and, without a lateral component, does not result in particle transport. If the beam is asymmetric in the back focal plane of the microscope objective, the back reflection is no longer perpendicular to the scan line, as shown in Fig. 4. This creates a lateral component of the radiation-pressure induced scattering force. Any such asymmetry, such as cutting the beam from one side, changes the average angle of incidence  $\theta$  of the focused laser light onto the microsphere. We use the average angle  $\theta$ , determined by the center of gravity of the intensity distribution in the back focal plane of the microscope objective, to esti-

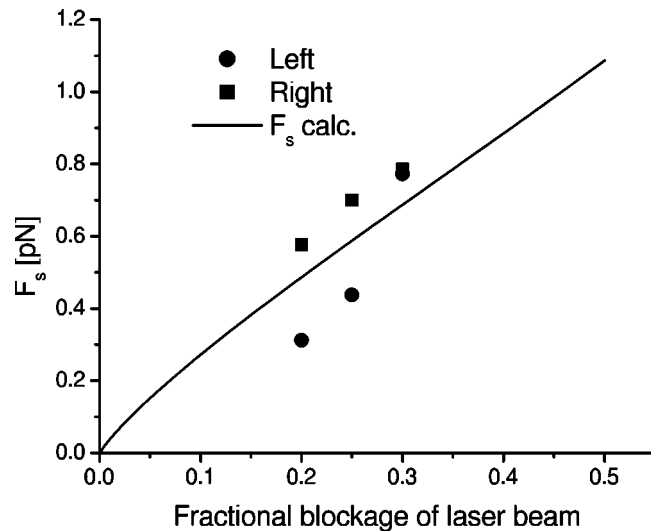


FIG. 5. Measured and calculated values for the lateral component of the scattering force. The experimental values were determined from the velocities of the motion shown in Fig. 2(a) and are compared to the predictions from Eq. (1).

mate the strength and direction of the lateral scattering force. We calculate this force by modifying the standard expression for the radiation-pressure induced force on a reflecting surface, and obtain

$$F_s(\theta) = 2 \frac{PR}{c} \sin \theta, \quad (1)$$

where  $P$  is the average incident laser power illuminating the microsphere, and  $R$  the Fresnel coefficient for reflection at normal incidence, using a refractive index of  $n = 1.59$  for the polystyrene bead and  $n = 1.33$  for the surrounding aqueous solution. Since the laser beam illuminates the microsphere only for a fraction of the scan period, we assume that on average 10% of the total laser power is incident on the microsphere. With these parameters we can calculate the expected force acting on the particle as a function of the fractional blockage of the beam in the back focal plane. A comparison of this computation with the observed forces, as determined from the velocities from Fig. 2(a), is shown in Fig. 5. The model agrees well with our experimental observations. It explains not only the scan direction and velocity independent lateral force on the microsphere, but also yields good quantitative results.

To directly measure the lateral scattering forces, we measured the escape forces for a particle in a stationary trap without the scanning modulator, in and against the direction of the scattering force. Experimentally, this was accomplished by applying a constant acceleration to the sample cell. This creates a linearly increasing friction force on the microsphere, until the trap, which has an intensity of  $\approx 30$  mW at the back focal plane, can no longer hold the particle. The velocity at which this happens was determined by fluorescence video microscopy. Special care was taken to ensure that the trap remained at a constant depth of  $10 \mu\text{m}$  above the cover slip while the stage is in motion, avoiding

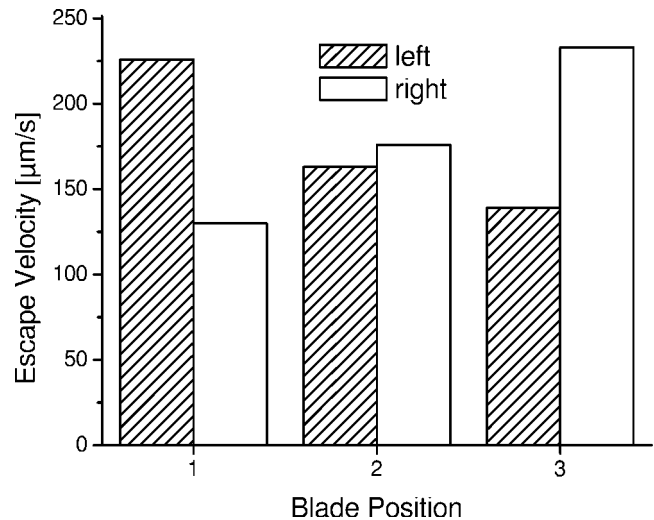


FIG. 6. Escape velocities of a microsphere from the stationary optical trap. (1) Blocking 49% of the laser beam from the right, (2) not blocking the beam, and (3) blocking 49% from the left.

any artifacts from a change in trap stiffness due to its axial location in the cell. The results for two strongly asymmetric beam profiles and a symmetric trap are shown in Fig. 6. For the symmetric trap, the escape velocities are about equal in both directions, while the asymmetric beam profiles reduce the escape velocities in the direction of the weakened side of the beam. This is consistent with the radiation-pressure model described above and in Fig. 4.

The model of a constant lateral radiation pressure on the microsphere can also be tested by mapping the force acting on a trapped particle as a function of its displacement in the trap. For this aim, we used the same constant-acceleration technique as described above to apply an increasing viscous drag force to the microsphere. As before, the displacement was measured by fluorescence video microscopy, while the force was inferred from the velocity of the microscope stage. The expected force-displacement relationship, the derivative of a Gaussian potential, was fitted to the data, with an additional offset  $x_0$  in the displacement that allows for a constant lateral force, such as the proposed radiation pressure force,

$$F(x) = \frac{A}{\sigma^2} (x - x_0) e^{-(x - x_0)^2 / 2\sigma^2} + F_0, \quad (2)$$

where  $A$  is the depth of the potential,  $\sigma$  the waist of the beam, and  $F_0$  the force offset corresponding to  $x_0$ .

The result for one representative curve with a beam asymmetry corresponding to a blockage of 49% of the laser beam is shown in Fig. 7. The experimental data agree extremely well with the theoretical prediction, except for forces right at the escape velocity. This indicates that the optical potential is indeed nearly Gaussian with very little asymmetry in the focal plane of the microscope objective, but shifted by the additional radiation-pressure force. The displacement in the absence of an external drag force, as determined from the fit, is  $x_0 = -50$  nm, which corresponds to a lateral radiation

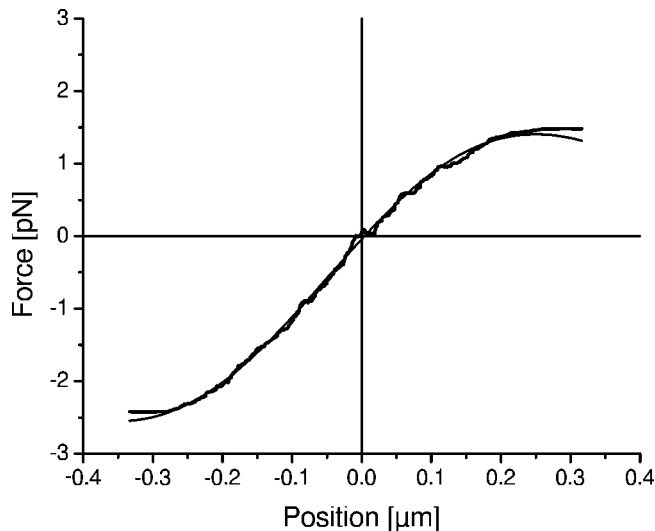


FIG. 7. Force-displacement curve of a bead in a stationary trap with an asymmetry of 49% in the back focal plane [compare column (1) in Fig. 6]. Experimental data are shown as the bold line (running average over 10 data points, 510 data points in total), together with a fit to the theoretical prediction of Eq. (2).

pressure force of  $F_0 = -0.57$  pN, which is consistent with our model and the observed particle velocities for these parameters.

The fact that the optical potential in the focal plane is symmetric and nearly Gaussian can be explained in the framework of Fourier optics. The electric field in the back focal plane is described by a Gaussian of width  $\omega_0$  that is cut off at  $x = b$ ,

$$E(x) \sim e^{-x^2/\omega_0^2} \Theta(b-x). \quad (3)$$

Then the electric field in the focal plane of the microscope objective with focal length  $f$  is given by the Fourier transform of  $E$ ,

$$\tilde{E}(x) \sim e^{-(m\omega_0/\lambda f)^2 x^2} \omega_n^2 \left[ 1 + \operatorname{erf} \left( \frac{b}{\omega_0} - i \frac{\pi \omega_0 x}{\lambda f} \right) \right]. \quad (4)$$

Noting that  $\tilde{E}(-x) = \tilde{E}^*(x)$ , we find that the intensity  $|\tilde{E}(x)|^2$  is symmetric with respect to the optical axis, as shown in our experiment. A numerical calculation of the potential that corresponds to Eq. (4) shows that this potential is indeed nearly Gaussian in the central region. At 49% beam blockage, it has a width of 550 nm as compared to a width of 430 nm for the potential corresponding to the unblocked beam. This is consistent with the data shown in Fig. 7, as well as the observation that the trap stiffness decreases with increasing beam blockage, as shown in Fig. 3(a).

#### IV. CONCLUSIONS

In conclusion, we have demonstrated that an asymmetric beam profile in the back focal plane of scanning-line optical tweezers can exert a substantial, approximately constant lateral force on a trapped particle over the entire length of the scan line of almost  $10 \mu\text{m}$ . This force is substantially larger than the forces arising from the scanning motion of the optical potential itself or from variations of the trap stiffness along the scan line and is independent of the scan direction or velocity. This force can be quantitatively understood in a simple geometric optics model and attributed to a lateral component in the radiation pressure exerted onto the particle by the light that is scattered back from it. Such a constant-force optical tweezing scheme may have important applications for the study of biological systems under constant-force conditions and eliminate the need for feedback tweezer systems.

#### ACKNOWLEDGMENTS

This work was supported by the National Institutes of Health through Grant No. GM69534, the Alfred P. Sloan Foundation, the National Science Foundation under Grant No. PHY0114336, and the Studienstiftung des deutschen Volkes.

- 
- [1] J.C. Meiners and S.R. Quake, *Phys. Rev. Lett.* **84**, 5014 (2000).  
 [2] M.S.Z. Kellermeyer, S.B. Smith, H.L. Granzier, and C. Bustamante, *Science* **276**, 112 (1997).  
 [3] M.D. Wang, M.J. Schnitzer, R.L.H. Yin, J. Gelles, and S.M. Block, *Science* **282**, 902 (1998).  
 [4] D.E. Smith, S.J. Tans, S.B. Smith, S. Grimes, D.L. Anderson, and C. Bustamante, *Nature (London)* **431**, 748 (2001).  
 [5] M.D. Wang, H. Yin, R. Landick, J. Gelles, and S.M. Block, *Biophys. J.* **72**, 1335 (1997).  
 [6] J.C. Crocker, J.A. Matteo, A.D. Dinsmore, and A.G. Yodh,

- Phys. Rev. Lett.* **82**, 4352 (1999).  
 [7] R.J. Owen, J.C. Crocker, R. Verma, and A.G. Yodh, *Phys. Rev. E* **64**, 011401 (2001).  
 [8] R. Verma, J.C. Crocker, T.C. Lubensky, and A.G. Yodh, *Macromolecules* **33**, 177 (2000).  
 [9] L.P. Faucheux, L.S. Bourdieu, P.D. Kaplan, and A.J. Libchaber, *Phys. Rev. Lett.* **74**, 1504 (1995).  
 [10] L.P. Faucheux, G. Stolovitzky, and A.J. Libchaber, *Phys. Rev. E* **51**, 5239 (1995).  
 [11] R. Nambiar and J.C. Meiners, *Opt. Lett.* **27**, 836 (2002).  
 [12] J.C. Meiners and S.R. Quake, *Phys. Rev. Lett.* **82**, 2211 (1999).